J|A|C|S
ARTICLES
Published on Web 10/30/2002

Energetic Contributions for the Formation of TAT/TAT, TAT/CGC$^+$, and CGC$^+$/CGC$^+$ Base Triplet Stacks

Ana Maria Soto,[†,||] Jacqueline Loo, and Luis A. Marky*[,†,‡,§]

Contributions from the Department of Pharmaceutical Sciences, Department of Biochemistry and Molecular Biology, and Eppley Institute for Cancer Research, University of Nebraska Medical Center, 986025 Nebraska Medical Center, Omaha, Nebraska 68198-6025

Received May 17, 2002

Abstract: We used a combination of spectroscopic and calorimetric techniques to determine complete thermodynamic profiles accompanying the folding of a set of triple helices and control duplexes. Specifically, we studied the sequences: d($A_7C_5T_7C_5T_7$), d($A_6C_5T_6C_5T_6$), d($A_6C_5T_6$), d(AGAGAGAC$_5$TCTCTCTC$_5$TCTCTCT), d(AGAGAC$_5$TCTCTC$_5$TCTCT), d(AGAGAC$_5$TCTCTC$_2$), d(AAGGAC$_5$TCCTTC$_5$TTCCT), d(AGGAAC$_5$TTCCTC$_5$TCCTT), and d(GAAAGC$_5$CTTTCC$_5$CTTTC). Circular dichroism spectroscopy indicated that all triplexes and duplexes are in the "B" conformation. DSC melting experiments revealed that the formation of triplexes is accompanied by a favorable free energy change, which arises from the compensation of a large and favorable enthalpic contribution with an unfavorable entropic contribution. Comparison of the thermodynamic profiles of these triplexes yielded enthalpic contributions of −24 kcal/mol, −23 kcal/mol, and −22 kcal/mol for the formation of TAT/TAT, TAT/CGC$^+$, and CGC$^+$/CGC$^+$ base triplet stacks, respectively. UV melts as a function of sodium concentration show sodium ions stabilize the triplexes that contain only TAT triplets but destabilize the triplexes that contain CGC$^+$ triplets. UV melts as a function of pH indicate that the protonation of the third strand and loop cytosines stabilizes the triplexes that contain CGC$^+$ and TAT triplets, respectively. Our overall results suggest that the triplex to duplex transition of triplexes that contain CGC$^+$ triplets is accompanied by a release of protons and an uptake of sodium, while their duplex to random coil transition is accompanied by a release of sodium ions. A consequence of this opposite sodium dependence is that their coupled transitions are nearly independent of sodium concentration but are dependent on the experimental pH.

Introduction

The completion of the human genome project will extensively change the pattern and focus of the research in pharmaceutical sciences.[1] Future analysis of the human genome may provide a number of potential gene targets that could be exploited for the development of therapeutic drugs.[1] Moreover, a number of point mutations or genetic polymorphisms are likely to be identified, making it imperative to produce drugs that offer a means to discriminate sequences that differ in only a few base pairs. Nucleic acid oligonucleotides, as drugs, present an exquisite selectivity and are able to discriminate targets that differ in a single base.[2] Therefore, oligonucleotides (ODNs) may be used to control gene expression.[3−5] There are two main approaches for the use of ODNs as modulators of gene expression: the antisense strategy and the antigene strategy.[3] In the antisense strategy, ODNs bind to messenger RNA, forming DNA/RNA hybrid duplexes. The formation of these hybrids inhibits translation by sterically blocking the correct assembly of the translation machinery or by inducing an RNAse H mediated cleavage of their mRNA target.[3] In the antigene strategy, ODNs bind to the major groove of a DNA duplex, forming triple helices.[6,7] The formation of triplexes can inhibit transcription by competing with the binding of proteins that activate the transcription machinery.[4,8]

By directly targeting the gene, the antigene strategy offers some advantages over the antisense strategy. First of all, there are only two copies of the gene, whereas there is a large continuous supply of the mRNA gene transcript. Moreover, blocking the transcription of the gene itself prevents repopulation of the mRNA pool, allowing a more efficient and lasting inhibition of gene expression.[5] On the other hand, one disadvantage is that the ODN needs to cross the nuclear membrane

* To whom inquires should be addressed. Telephone: (402) 559-4628. Fax: (402) 559-9543. E-mail: lmarky@unmc.edu.
[†] Department of Pharmaceutical Sciences, University of Nebraska Medical Center.
[‡] Department of Biochemistry and Molecular Biology, University of Nebraska Medical Center.
[§] Eppley Institute for Cancer Research, University of Nebraska Medical Center.
[||] Present Address: Department of Chemistry, Johns Hopkins University, Baltimore, MD 21218.

(1) Juliano, R. L.; Astriab-Fisher, A.; Falke, D. *Mol. Interventions*, **2001**, *1*, 40−53.
(2) Crooke, S. T. *Biochim. Biophys. Acta* **1999**, *1489*, 31−44.
(3) Helene, C. *Eur. J. Cancer* **1991**, *27*, 1466−1471.
(4) Helene, C. *Eur. J. Cancer* **1994**, *30A*, 1721−1726.
(5) Praseuth, D.; Guieysse, A. L.; Helene, C. *Biochim. Biophys. Acta* **1999**, *1489*, 181−206.
(6) Soyfer, V. N.; Potaman, V. N. *Triple-Helical Nucleic Acids;* Springer-Verlag: New York, 1996.
(7) Thuong, N. T.; Helene, C. *Angew. Chem., Int. Ed.* **1993**, *32*, 666−690.
(8) Maher, L. J., III; Wold, B.; Dervan, P. B. *Science* **1989**, *245*, 725−730.

Scheme 1. TAT and CGC$^+$ Base Triplets

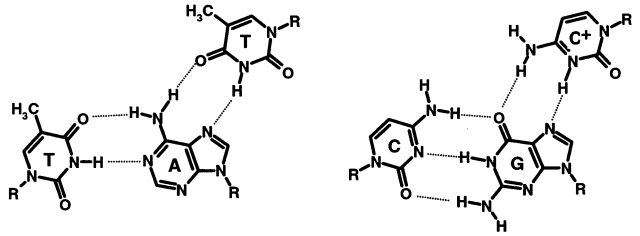

and access its DNA target within the densely packed chromatin structure.[9,10]

The formation of triplexes is sequence specific, allowing the recognition of different DNA sequences by Hoogsteen base pairing.[6,7] Triplexes are stabilized by base triplet stacking interactions and hydrogen bonding between the third strand bases and purine bases of the duplex.[11] Triplexes can be classified on the basis of the composition and/or orientation of the third strand. Parallel triplexes are usually pyrimidine rich and bind parallel to the purine strand of the duplex, while antiparallel triplexes are usually purine rich and bind the duplex purine strand in the antiparallel orientation.[6,12,13] Parallel triplexes are characterized by the formation of T•A*T and C•G*C$^+$ base triplets ("•" and "*" represent Watson−Crick and Hoogsteen base pairing, respectively). These triplets are isomorphous, that is, super imposable, allowing a regular conformation of the sugar−phosphate backbone.[6] However, triplexes containing different combinations of these triplets have been shown to exhibit different stabilities.[13] Successful control of gene expression depends on the effective binding of a specific DNA sequence. Therefore, to develop triplexes as therapeutic agents, it is imperative to have a clear understanding of how the sequence, base composition, and solution conditions affect the stability of these molecules. To this end, we have studied a set of intramolecular triplexes, with different nucleotide sequences and composition. The use of intramolecular structures simplifies the study of triple helices because they are more stable than their bimolecular and trimolecular counterparts.[14] Moreover, they resemble the intramolecular structure of H-DNA, a structure that has been detected in eukaryotic and prokaryotic cells and that is thought to play a role in chromatin structure.[5,6]

In this work, we have used a combination of optical and calorimetric techniques to study the stability of a set of triplexes that contain T•A*T and C•G*C$^+$ base triplets, shown in Scheme 1, in a variety of solution conditions. Our results show that the formation of each base triplet stack is driven by a large and favorable enthalpic contribution and that optimized solution conditions for a given sequence can be chosen on the basis of the nucleotide sequence and composition of the resulting triplex. Moreover, our results offer a reasonable hypothesis for the unfolding of intramolecular triplexes, which includes the effects of ions and pH. Our results suggest that the large and unfavorable ΔH of unfolding the third strand is not compensated by the small favorable entropy change of releasing the third strand from these intramolecular triplexes. Factors that increase

Scheme 2. Structures of Duplexes and Triplexes[a]

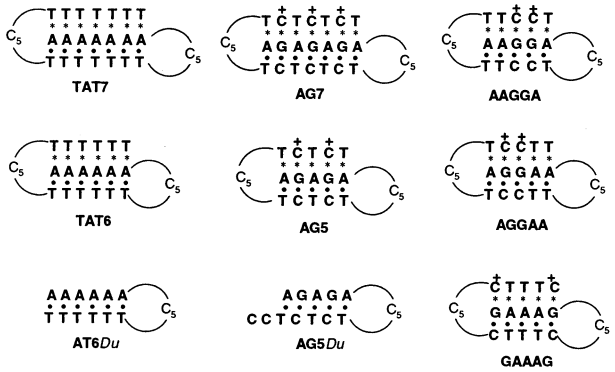

[a] The suffix *Du* denotes a duplex, while the remaining molecules are in the triplex state.

the ΔS of unfolding, such as the uptake of counterions observed in triplexes containing CGC$^+$ triplets or an increase in the triplex length, promote the biphasic unfolding of intramolecular triplexes. Our analysis not only elucidates the pH and cation dependence in the unfolding of intramolecular triplexes but also helps in the design of triplexes as therapeutic agents in at least two ways. First, they will allow researchers to select the target gene sequences that are more likely to form a stable triplex, given the environmental conditions of the cell nucleus. Second, they will allow the selection of the appropriate solution conditions for the formation of a given triple helix sequence for *in vitro* experiments.

Materials and Methods

Materials. All oligonucleotides were synthesized by the Core Synthetic Facility of the Eppley Research Institute at University of Nebraska Medical Center, HPLC purified, and desalted by column chromatography. The concentration of the oligomer solutions was determined at 260 nm and 80 °C using the following molar extinction coefficients in mM^{-1} cm^{-1} of strands: $^{5'-}d(A_7C_5T_7C_5T_7)^{-3'}$, 273; $^{5'-}d(A_6C_5T_6C_5T_6)^{-3'}$, 246; $^{5'-}d(A_6C_5T_6)^{-3'}$, 162; $^{5'-}d(AGAGAC_5TCTCTC_5TCTCT)^{-3'}$, 210; $^{5'-}d(AGAGAGAC_5TCTCTCTC_5TCTCTCT)^{-3'}$, 266; $^{5'-}d(AGAGAC_5TCTCTC_2)^{-3'}$, 151; $^{5'-}d(AGGAAC_5TTCCTC_5TCCTT)^{-3'}$, 209; $^{5'-}d(AAGGAC_5TCCTTC_5TTCCT)^{-3'}$, 209; $^{5'-}d(GAAAGC_5CTTTCC_5CTTTC)^{-3'}$, 207. These values were calculated by the extrapolation of the tabulated values of the dimmers and monomer bases[15] at 25 °C to high temperatures, using procedures reported earlier.[16] Buffer solutions consisted of 10 mM sodium cacodylate or 10 mM sodium phosphate, adjusted to different sodium concentrations and pH with NaCl and HCl, respectively. All molecules and their corresponding designations are shown in Scheme 2.

Circular Dichroism (CD). Evaluation of the conformation of each duplex or triplex was obtained by simple inspection of their CD spectrum. These spectra were obtained on an AVIV circular dichroism spectrometer model 202-SF (Lakewood, NJ), using a 10-mm quartz cuvette. All spectra were collected at 0 °C, between 200 and 400 nm, using a wavelength step of 1 nm. The reported spectra represent the average of at least two scans.

Temperature-Dependent UV Spectroscopy (UV Melts). Absorbance versus temperature profiles (melting curves) for each duplex and triplex were measured at 260 nm with a thermoelectrically controlled Aviv 14-DS spectrophotometer, as a function of strand, pH, and salt concentration. The temperature was scanned at a heating rate of ∼0.6 °C/min. These melting curves allow us to measure transition temper-

(9) Brown, P. M.; Madden, C. A.; Fox, K. R. *Biochemistry* **1998**, *37*, 16139−16151.
(10) Neidle, S. *Anti-Cancer Drug Des.* **1997**, *12*, 433−442.
(11) Cheng, Y. K.; Pettitt, B. M. *Prog. Biophys. Mol. Biol.* **1992**, *58*, 225−257.
(12) Beal, P. A.; Dervan, P. B. *Science* **1991**, *251*, 1360−1363.
(13) Keppler, M. D.; Fox, K. R. *Nucleic Acids Res.* **1997**, *25*, 4644−4649.
(14) Chen, F. M. *Biochemistry* **1991**, *30*, 4472−4479.
(15) Cantor, C. R.; Warshaw, M. M.; Shapiro, H. *Biopolymers* **1970**, *9*, 1059−1077.
(16) Marky, L. A.; Blumenfeld, K. S.; Kozlowski, S.; Breslauer, K. J. *Biopolymers* **1983**, *22*, 1247−1257.

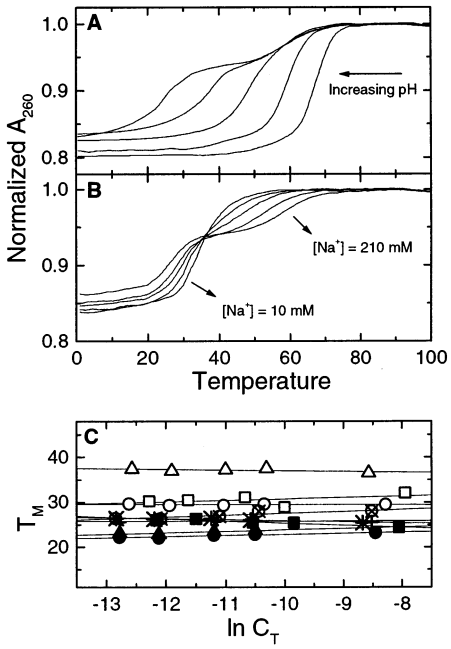

Figure 1. (A) UV melting curves of AG7 as a function of pH, in 10 mM sodium cacodylate and 200 mM sodium chloride; curves correspond to pH values of 5.2, 5.7, 6.2, 6.7, and 7.2. (B) UV melting curves of AG7 as a function of sodium concentration, in 10 mM sodium cacodylate, at pH 7.2, are shown; curves correspond to sodium concentrations of 10, 21, 46, 98, and 210 mM. (C) T_M dependence on strand concentration is shown for TAT7 (▲), TAT6 (●), AT6*Du* (■), AG7 (△), AG5 (○), AG5*Du* (□), AAGGA (★), AGGAA (+), and GAAAG (⊗).

atures, T_M, which are the midpoint temperatures of the order−disorder transition of the duplexes and triplexes, van't Hoff enthalpies, ΔH_{vH}, using a two-state transition approximation, as reported previously,[17] and the thermodynamic release of protons, Δn_{H^+}, and counterions, Δn_{Na^+}.

Differential Scanning Calorimetry (DSC). To investigate the helix coil transition of each oligomer, excess heat capacities as a function of temperature (melting curves) were measured with a Microcal MC-2- or VP-differential scanning calorimeters (Northampton, MA). Two cells, the sample cell containing 1.6 mL (MC-2) or 0.8 mL (VP) of oligomer solution and the reference cell filled with the same volume of buffer solution, were heated from 0 to 90 °C at a heating rate of 0.75 °C/min. Analysis of the resulting thermograms, using procedures described previously, yields standard thermodynamic profiles (ΔH_{cal}, ΔS_{cal}, ΔC_p, and $\Delta G°_{cal}$) and model-dependent van't Hoff enthalpies, ΔH_{vH}, for the transition of each hairpin.

Results

UV Melts. UV melting experiments were conducted at different salt and pH conditions and were used to characterize the helix−coil transition of the duplexes and triplexes, shown in Scheme 2. Figure 1 shows typical melting curves; above 10 °C, all curves follow the characteristic sigmoidal behavior for the unfolding of a nucleic acid helix. The UV melts of the control duplexes and of the triplexes that contain only TAT base triplets exhibit monophasic transitions under all conditions, consistent with previous reports.[18,19] In contrast, the triplexes that contain CGC^+ triplets melt in monophasic or biphasic transitions, depending on solution conditions. At low sodium concentrations and acidic pH, these triplexes exhibit monophasic transitions, while, at basic pH and high sodium concentrations, we observed biphasic transitions. The UV melts of AG7, shown in Figure 1, illustrate this effect. UV melts at different total strand concentrations were conducted to determine the T_M dependence on strand concentration and van't Hoff enthalpies, ΔH_{vH}. The T_M dependence on strand concentration for the unfolding of each molecule is shown in Figure 1c. Over a 50-fold concentration range, the T_M values of all molecules are independent of strand concentration, confirming the formation of intramolecular structures. We used the relationship $\Delta H_{vH} = 4RT_M2\ \partial\alpha/\partial T$,[17] to calculate the ΔH_{vH}^{Shape} values, shown in the last column of Table 1; these values represent the average of at least seven melting curves. The van't Hoff enthalpies of TAT7, TAT6, AT6*Du*, AG5, and AG5*Du* were found to be independent of pH or sodium concentration, while, for the remaining triplexes, they depended on the experimental pH, with larger values on the pH range of 5.2−6.2 and smaller values in the pH range of 6.7−7.2.

Circular Dichroism. The CD spectra of each molecule are shown in Figure 2. The triplexes TAT7 and TAT6 as well as the control duplexes exhibit the typical spectra of a nucleic acid duplex in the "B" conformation; that is, the positive band centered at ~278 nm has a similar magnitude to the negative band at ~245 nm. The triplexes AG5, AG7, AGGAA, AAGGA, and GAAAG also adopted the "B" conformation, although their CD spectra presented some deviations from the typical "B" conformation, including an overall shift of the spectra toward higher wavelengths. These deviations may be the result of the presence of protonated cytosines in the stem of these molecules. All triplexes showed a band at 210 nm with larger magnitudes than that of duplex DNA, which may be characteristic for the formation of triple helices.

Differential Scanning Calorimetry. The DSC melting curves of each oligonucleotide are shown in Figure 3, and the thermodynamic profiles determined from these curves at 5 °C are summarized in Table 1. The ΔH_{cal} and ΔS_{cal} parameters were measured directly using the equations $\Delta H_{cal} = \int \Delta C_p{}^a\, dT$ and $\Delta S_{cal} = \int (\Delta C_p{}^a/T) dT$, where $\Delta C_p{}^a$ represents the anomolous heat capacity during the unfolding process. We measured heat capacity effects ranging from 0 to 75 cal/mol °C; however, these heat capacity effects are considered small enough and can be ignored without compromising the overall trend of the results. The free energy change at 5 °C, $\Delta G°_{278}$, is obtained from the Gibbs equation: $\Delta G°_{278} = \Delta H_{cal} - T\Delta S_{cal}$. Table 1 also shows van't Hoff enthalpies calculated from the shape of the DSC curves. These enthalpies are similar to the ones obtained from analysis of the UV melting curves. The $\Delta H_{vH}/\Delta H_{cal}$ ratios of 1.08−1.13 obtained for the duplexes indicate that these molecules unfold in two-state transitions; that is, the transitions occur in an all-or-none fashion without the presence of intermediate states. The large difference between van't Hoff and calorimetric enthalpies obtained for each triplex indicates that these molecules unfold in non-two-state transitions and suggests the presence of coupled transitions with similar T_M. Inspection of Table 1 reveals that triplex or duplex folding at 5 °C is accompanied by a favorable free energy term resulting from the characteristic compensation of favorable enthalpy and unfavorable entropy terms. In general, these favorable enthalpy terms mainly correspond to heat contributions from the formation of base−base stacking interactions, while the unfavorable

(17) Marky, L. A.; Breslauer, K. J. *Biopolymers* **1987**, *26*, 1601−1620.
(18) Rentzeperis, D. Doctoral Dissertation, New York University, New York, 1994.
(19) Rentzeperis, D.; Marky, L. A. *J. Am. Chem. Soc.* **1995**, *117*, 5423−5424.

Table 1. Thermodynamic Profiles for the Formation of Triplexes and Duplexes at 5 °C[a]

	pH	[Na^+] (mM)	T_M (°C)	$\Delta G°$ (kcal/mol)	ΔH_{cal} (kcal/mol)	$T\Delta S$ (kcal/mol)	ΔH_{vH} (kcal/mol)	ΔH_{vH}^{Shape} (kcal/mol)
TAT7	7	16	23.2	−5.8	−93.9	−88.1	−53	
		116	34.8	−9.0	−92.9	−83.9	−49	−51
		1116	53.8	−12.7	−85.3	−72.6	−58	
TAT6	7	16	20.6	−3.7	−69.5	−65.8	−54	
		116	30.2	−6.0	−71.6	−65.7	−50	−48
		200	33.7	−6.6	−70.9	−64.3	−48	
		1116	47.0	−8.0	−61.1	−53.1	−49	
AT6*Du*	7	16	24.3	−2.3	−35.1	−32.8	−38	−33
		1116	45.0	−3.8	−30.3	−26.5	−33	
AG7	7	16	37.3	−10.9	−104.7	−93.8	−37	−52
	6.2	10	52.6	−19.1	−130.7	−111.6	−70	−77
AG5	7	16	29.3	−5.6	−69.3	−63.7	−49	−52
	6.2	10	43.0	−10.2	−84.8	−74.6	−53	
AG5*Du*	7	16	31.9	−2.6	−29.2	−26.6	−33	−31
AAGGA	7	16	25.4	−3.7	−54.4	−50.7	−42	−48
	6.2	10	42.8	−11.3	−94.6	−83.3	−58	−61
AGGAA	7	16	25.5	−4.0	−58.9	−54.9	−43	−50
	6.2	10	44.0	−11.0	−89.6	−78.6	−57	−64
GAAAG	7	16	27.9	−3.6	−47.6	−44.0	−34	−43
	6.2	10	41.8	−10.0	−85.9	−75.9	−47	−53

[a] Experiments were conducted in 10 mM sodium phosphate buffer, at pH 7.0, or 10 mM sodium cacodylate buffer, at pH 6.2. The ΔH_{vH} and ΔH_{vH}^{Shape} terms are obtained from the shape of calorimetric and UV melting curves, respectively. T_M values are within 0.5 °C, ΔH_{cal} values are within 3%, $\Delta G°$ and $T\Delta S$ values are within 5%, and ΔH_{vH} and ΔH_{vH}^{Shape} are within 10%.

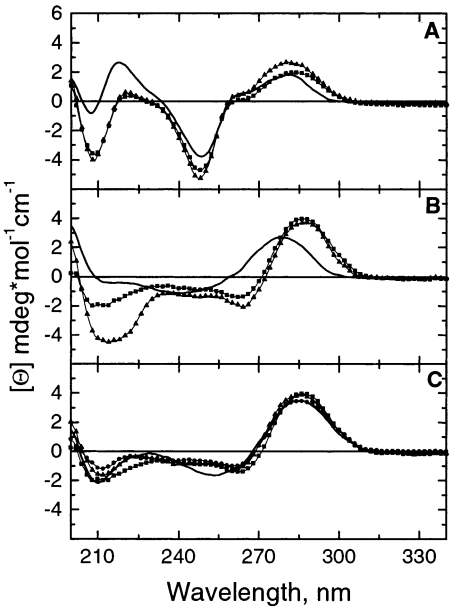

Figure 2. Circular dichroism spectra of triplexes and duplexes. (A) Spectra of TAT7 (▲), TAT6 (■), and AT6*Du* (−) in 10 mM sodium phosphate, at pH 7, are shown. (B) Spectra of AG7 (▲), AG5 (■), and AG5*Du* (−) in 10 mM sodium cacodylate, at pH 6.2, are shown. (C) Spectra of AG5 (■), AAGGA (▲), AGGAA (●), and GAAAG (−) in 10 mM sodium cacodylate, at pH 6.2, are shown.

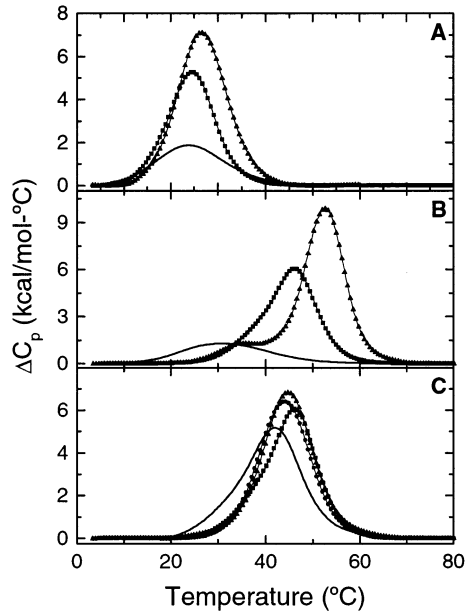

Figure 3. Typical DSC curves of triplexes and duplexes. (A) Curves for TAT7 (▲), TAT6 (■), and AT6*Du* (−) in 10 mM sodium phosphate, at pH 7, are shown. (B) Curves for AG7 (▲), AG5 (■), and AG5*Du* (−) in 10 mM sodium cacodylate, at pH 6.2, are shown. (C) AG5 (■), AAGGA (▲), AGGAA (●), and GAAAG (−) in 10 mM sodium cacodylate, at pH 6.2, are shown.

entropy terms arise from contributions of the unfavorable ordering of strands and the uptake of counterions, protons, and water molecules. Closer inspection of Table 1 reveals that the triplexes in each set unfold with larger enthalpies, relative to the corresponding control duplexes. This is consistent with the incorporation of a third strand. In addition and as expected, the longer triplexes (TAT7 and AG7) with seven base triplets unfold with larger enthalpies compared with those of the shorter triplexes (TAT6 and AG5) containing five to six base triplets consistent with the addition of one and two base triplet stacks, respectively.

As shown in Table 1, the stabilities (T_M and $\Delta G°$) of the triplexes containing only TAT triplets increase as the sodium concentration increases. This is consistent with a better screening of the negatively charged phosphates at higher ionic strengths. In addition, their enthalpy values appear to be independent of salt concentration and decrease only at very high sodium concentrations.

The stability of the triplexes containing CGC^+ triplets increases with decreasing pH. This stabilization is accompanied by an enthalpy increase, suggesting that low pH is required for the optimum formation of the base triplet stacking interactions of these molecules.

Furthermore, the difference in enthalpies at pH 6.2 and 7.0 is larger for the triplexes containing consecutive cytosines (AAGGA and AGGAA) or cytosines next to the loops (GAAAG).

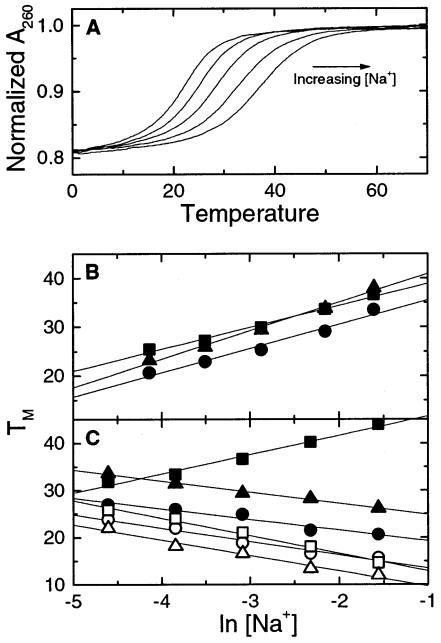

Figure 4. (A) UV melting curves of TAT7 over a NaCl concentration range of 16−200 mM, in 10 mM sodium phosphate, pH 7.0, at a constant strand concentration of 5 μM; curves correspond to sodium concentrations of 16, 30, 57, 116, and 200 mM. (B) T_M dependence on salt concentration is shown for TAT7 (▲), TAT6 (●), and AT6*Du* (■). (C) T_M dependence on salt concentration is shown for AG7 (▲), AG5 (●), AG5*Du* (■), AAGGA (○), AGGAA (□), and GAAAG (△).

This is consistent with previous reports[20] and reflects the importance of cytosine protonation in the formation of CGC^+ triplets.

Thermodynamic Release of Counterions. UV melting curves at several salt concentrations and the T_M dependence on salt concentration are shown in Figure 4. The thermodynamic release of counterions, $\Delta n_{Na}{}^+$, is determined from the equation $\Delta n_{Na}{}^+ = -1.11(\Delta H_{cal}/RT_M{}^2)\ \partial T_M/\partial \ln[Na^+]$,[21] where the $\partial T_M/\partial \ln[Na^+]$ term corresponds to the slope of T_M versus $\ln[Na^+]$ plots, the term in parentheses is obtained in DSC melting experiments, R is the universal gas constant, and 1.11 is a proportionality constant for converting concentrations into ionic activities. The $\Delta n_{Na}{}^+$ values were calculated using the slopes of the T_M dependence on sodium at pH 5.2 and 7.2. The enthalpy values used correspond to the formation of a particular base stack at that pH (i.e., the heats obtained at pH 6.2 or 7.0 for the triplexes containing CGC^+ triplets and the heats obtained at low sodium concentrations for the remaining molecules). The resulting $\Delta n_{Na}{}^+$ values are summarized in Table 2. At pH 7.2, the duplexes and the "TAT triplexes", triplexes containing only TAT base triplets, yielded a net uptake of counterions. This is consistent with the higher charge density of the folded nucleic acid structures relative to the unfolded states. However, the folding of the "CGC^+ triplexes", triplexes with CGC^+ triplets, releases counterions. This probably reflects the protonation of the third strand cytosines, which exclude sodium from the stem of these molecules. At the lower pH of 5.2, the duplexes and the "TAT triplexes" take up counterions in smaller amounts (by ∼0.9 mol of Na^+/mol of triplex) than at pH 7.2. At this low pH, the "CGC^+ triplexes" exhibit a decreased release of sodium ions. This decrease is so marked that, in most cases, it reverses the release of counterions observed at pH 7.2 to an uptake of counterions at pH 5.2. However, the overall uptake or release observed at pH 5.2 is very small and, in most of the cases, may be considered negligible. Thus, at pH 5.2, the formation of "CGC^+ triplexes" may be considered independent of sodium concentration.

Table 2. Thermodynamic Uptake of Counterions upon Folding[a]

oligomer	pH	$\partial T_M/\partial \ln[Na^+]$ (°C)	Δn_{Na+} per mol of hairpin
TAT7	7	5.85	−3.50
	5.2	4.41	−2.44
TAT6	7	4.98	−2.25
	5.2	3.68	−1.50
AT6*Du*	7	4.50	−1.00
	5.2	2.06	−0.42
AG7	7	−2.36	1.45
	5.2	1.42	−0.92
AG5	7	−2.27	0.97
	5.2	0.24	−0.10
AG5*Du*	7	4.07	−0.71
	5.2	1.45	−0.25
AAGGA	7	−2.84	0.97
	5.2	−1.05	0.50
AGGAA	7	−3.73	1.38
	5.2	−0.15	0.07
GAAAG	7	−3.26	0.95
	5.2	0.84	−0.39

[a] Experiments were conducted in 10 mM sodium phosphate, at pH 7.0, or 10 mM sodium cacodylate buffer, at pH 5.2 or 7.2, and adjusted to different sodium concentrations by adding NaCl. $\partial T_M/\partial \ln[Na^+]$ values are within 4%, and Δn_{Na+} values are within 6%.

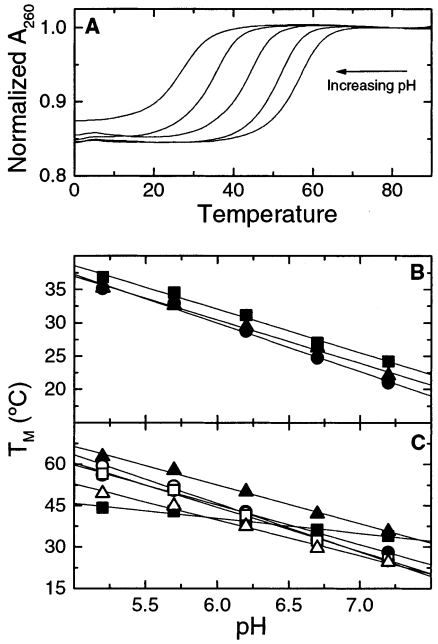

Figure 5. (A) UV melting curves of AG5 over a pH range of 5.2−7.2, in 10 mM sodium cacodylate, at a constant strand concentration of 5 μM; curves correspond to pH values of 5.2, 5.7, 6.2, 6.7, and 7.2. (B) T_M dependence on pH is shown for TAT7 (▲), TAT6 (●), and AT6*Du* (■). (C) T_M dependence on pH is shown AG7 (▲), AG5 (●), AG5*Du* (■), AAGGA (○), AGGAA (□), and GAAAG (△).

Thermodynamic Release of Protons. UV melting curves at several pH values are shown in Figure 5a, increasing the pH shifts of the curves toward higher temperatures. The T_M dependences on pH, shown in Figure 5b, allow us to estimate the thermodynamic release of protons, $\Delta n_H{}^+$. This parameter

(20) Leitner, D.; Schroder, W.; Weisz, K. *Biochemistry* **2000**, *39*, 5886−5892.
(21) Rentzeperis, D.; Kharakoz, D. P.; Marky, L. A. *Biochemistry*, **1991**, *30*, 6276−6283.

Table 3. Thermodynamic Uptake of Protons[a]

oligomer	[Na^+] (mM)	$\partial T_M/\partial$pH (°C)	Δn_{H^+} per mol of hairpin
TAT7	16	−6.50	−1.51
	210	−5.22	−1.10
TAT6	16	−7.28	−1.28
	200	−7.04	−1.16
AT6*Du*	16	−6.5	−0.63
	200	−4.62	−0.41
AG7	10	−14.00	−3.55
	210	−21.28	−5.84
AG5	10	−14.42	−2.68
	210	−19.66	−4.07
AG5*Du*	16	−5.44	−0.37
	210	−0.84	−0.06
AAGGA	10	−17.60	−3.65
	210	−20.92	−4.54
AGGAA	10	−16.02	−3.16
	210	−21.44	−4.36
GAAAG	10	−13.02	−2.54
	210	−20.36	−3.97

[a] Experiments were conducted in 10 mM sodium cacodylate buffer, adjusted to sodium concentrations of 10 mM or 210 mM with NaCl and to pH values in the range 5.2−7.2 with HCl. $\partial T_M/\partial$pH values are within 4%, and Δn_{H+} values are within 6%.

is determined using the following equation (similar to the one used to calculate $\Delta n_{Na}{}^+$): $\Delta n_{H}{}^+ = -0.434(\Delta H_{cal}/RT_M{}^2)\ \partial T_M/\partial$pH,[22,23] where $\partial T_M/\partial$pH corresponds to the slope of T_M versus pH plots, the term in parentheses is obtained in DSC experiments, and 0.434 is a proportionality constant for converting natural logarithms into decimal logarithms. The resulting $\Delta n_{H}{}^+$ values are shown in Table 3. At low sodium concentrations (10 mM), all molecules yieded a net uptake of protons. This uptake is relatively small for the duplexes and "TAT triplexes", reflecting the protonation of the cytosine loops. The "CGC^+ triplexes" take up protons in amounts that are larger than the number of the stem cytosines. This larger uptake of protons is consistent with the protonation of the third strand and loop cytosines. However, it is worth noticing that the excess of protons is particularly high in the case of AAGGA and AGGAA. At high sodium concentrations, the uptake of protons decreases for the "TAT triplexes" and control duplexes. In contrast, the "CGC^+ triplexes" exhibit a significant increase in the uptake of protons at higher sodium concentrations. These effects suggest that the presence of sodium decreases the pK_a of the cytosines located at the stem and loop of these triplexes.

Discussion

Triplex Design. All molecules were designed to fold into intramolecular structures. The use of intramolecular triplexes presents several advantages. First, they are more stable than their trimolecular counterparts because they form at a lower entropy cost. In addition, their folding takes place even at low sodium concentrations, allowing us to study their properties in a wide range of solution conditions. This is in contrast to intermolecular triplexes, which only form at very high salt concentrations or in the presence of divalent cations (including transition metal ions). As shown in Figure 1, the T_M values of all triplexes and duplexes are independent of strand concentration, confirming the exclusive formation of intramolecular hairpin loop structures.

To obtain thermodynamic contributions for the formation of particular base triplet stacks and for the incorporation of a third strand, the investigated duplexes and triplexes can be grouped into three sets. The first set includes the triplexes containing only TAT triplets, TAT7 & TAT6, and the control duplex AT6*Du*. TAT7 contains seven TAT triplets or six TAT/TAT base triplet stacks, while TAT6 contains six of such triplets or five base triplet stacks. Therefore, the comparison of TAT7 with TAT6 will give us the contributions for the incorporation of a TAT/TAT base triplet stack, while the comparison of TAT6 with AT6*Du* will give us the contributions for the incorporation of a third strand into a duplex. The second set includes the triplexes AG5 and AG7 and the control duplex AG5*Du*. These triplexes contain CGC^+ triplets interspaced by TAT triplets. The comparison between AG5 and AG7 will give us the thermodynamic contributions for the incorporation of one TAT and one CGC^+ triplets. This corresponds to the incorporation of two TAT/CGC^+ base triplet stacks, assuming that the contribution of the TAT/CGC^+ and CGC^+/TAT stacks are equivalent. The comparison of AG5 with AG5*Du* will give us the energetic contributions for the incorporation of a third strand into a duplex. The third set includes AAGGA, AGGAA, GAAAG, and AG5. All these triplexes contain two CGC^+ triplets and three TAT triplets but in different positions. Comparison between these molecules will help us understand the effect of sequence on the stability of triple helices. In addition, AAGGA and AGGAA incorporate CGC^+/CGC^+ base triplet stacks, allowing us to elucidate the contribution of this particular stack by comparing these triplexes with those of the previous two sets.

Circular Dichroism. CD spectroscopy shows that all triplexes retain the conformation of their parent duplex. This indicates that binding of the third strand does not impose major distortions in the duplex geometry. The CD spectra of the triplexes containing protonated cytosines in their stems are red shifted. The presence of a positive charge in the N4 of cytosine may alter the electron delocalization around the aromatic ring of this base and of the surrounding bases. This effect may be responsible for the absorbance shift observed in these molecules. Closer analysis of the CD spectra reveals that the triplexes exhibit an increased negative band at 210 nm, when compared with that of their control duplexes. This band has also been observed in previous reports[23] and may be a characteristic feature for the folding of triple helices.

Differential Scanning Calorimetry. The DSC experiments were conducted under a variety of salt and pH conditions. In the case of triplexes containing only TAT stacks, these experiments were conducted at different salt concentrations. In these experiments, we chose to maintain a constant pH of 7.0 because the formation of TAT base triplets does not involve any acid−base equilibrium and is expected to be independent of pH. As the sodium concentration increases, the stability of these triplexes increases, consistent with the higher screening of negative charges at higher sodium concentrations. This stabilization is entropic in origin and reflects the decreased sodium gradient between the local environment of the DNA and the bulk solution. When the sodium concentration was increased from 16 mM to 200 mM, their unfolding enthalpy remains constant, as expected for negligible heat contributions for salt effects.[24] The enthalpy decrease observed at 1.1 M NaCl

(22) Record, M. T., Jr.; Woodbury, C. P.; Lohman, T. M. *Biopolymers* **1976**, *15*, 893−915.
(23) Plum, G. E.; Breslauer, K. J. *J. Mol. Biol.* **1995**, *248*, 679−695.
(24) Krakauer, H. *Biopolymers* **1972**, *11*, 811−828.

probably reflects hydration changes that may occur in response to the effect of high sodium concentrations on the properties of the bulk solvent. In the case of triplexes containing CGC^+ triplets, the experiments were conducted at pH 7 and pH 6.2. NMR studies have shown that, below pH 6.5, the formation of triplexes containing protonated cytosines is nearly complete;[20,25,26] therefore, pH 6.2 was chosen as an ideal pH for the complete formation of these triplexes. Furthermore, NMR studies have also shown that a protonated cytosine in the third strand of a triplex has an average pK_a of ~7.[20] Therefore, ~87% of the cytosines should be protonated at pH 6.2, ensuring the complete formation of these triplexes. At the same time, pH 6.2 is high enough to avoid the presence of tautomeric conformations in the other bases, ensuring the appropriate formation of the duplex part of these molecules. Additional experiments were carried out at pH 7.0 to analyze the extent of triplex formation at physiologically more relevant conditions. The DSC melts indicate that, under these conditions, all triplexes melt in monophasic non-two-state transitions. In contrast, the control duplexes exhibit two-state transitions, which is consistent with their smaller size and simpler unfolding (duplex→random coil). The presence of non-two-state transitions in the triplexes can be explained by the presence of two coupled transitions: (a) triplex→duplex and b) duplex→random coil. Indeed, deconvolution of their transitions yields two all-or-none transitions with very similar T_M values (data not shown). Analysis of Table 1 reveals that the driving force for the formation of triplexes at 5 °C is a large and favorable enthalpy change. Comparison of the ΔH_{cal} values of the triplexes and the corresponding control duplexes yields enthalpic contributions of 35−50 kcal/mol for the incorporation of a third strand. This enthalpic contribution is too large to represent the exclusive formation of additional stacking interactions with the third strand. One possible explanation is that binding of the third strand optimizes the base stacking interactions of the duplex part of the triplex. This explanation is consistent with the results of the deconvolution analysis, which shows a larger than expected enthalpy for the duplex contributions of the molecule.

Thermodynamic Profiles for the Formation of Base Triplet Stacks. Comparison between the thermodynamic profiles of TAT6 and TAT7 yields an enthalpic contribution of −24.4 kcal/mol for the formation of a TAT/TAT base triplet stack. A similar comparison of AG5 and AG7 yields an enthalpic contribution of −23.0 kcal/mol for the incorporation of a TAT/CGC^+ base triplet stack. A similar comparison of the remaining parameters yields the $\Delta G°$ and $T\Delta S$ contributions for the formation of each base triplet stack. This comparison is possible because the only difference between the shorter and longer triplexes of these sets is the incorporation of additional base triplet stacks. Therefore, the additional contributions to $\Delta G°$ and $T\Delta S$ (nucleation, loops formation, etc.) are considered to be similar. The energetic contributions for the formation of these stacks are summarized in Table 4. The enthalpic contribution of each base triplet stack can also be calculated by dividing the ΔH_{cal} value of each molecule by the correspondent number of triplets in that molecule. This analysis yields a contribution of −13.9 kcal/mol to −15.7 kcal/mol for the formation of a TAT/TAT base triplet stack and a contribution of −21.5 kcal/mol for the formation of a TAT/CGC^+ base triplet stack. The apparent contradiction in the values of the TAT/TAT base triplet stacks may be explained by the presence of frayed ends. For instance, if we assume that the base stacks at either end do not form, we obtain a contribution of −23.3 kcal/mol for the formation of a TAT/TAT base stack. When all the triplexes of this study containing terminal TAT base triplets are considered, it is not clear why only the TAT7 and TAT6 triplexes present frayed ends. One possible explanation is that the presence of a neighboring CGC^+ triplet forces the terminal TAT to remain stacked in the helix. Support to this hypothesis comes from thermodynamic studies showing that the extent of fraying in duplexes containing only AT base pairs spreads over ~1.2 stacks at either end.[27] Incorporation of a single GC base pair in these duplexes completely abolished end fraying.[27] The higher stability of TAT/CGC^+ triplets is also consistent with this hypothesis. Indeed, closer analysis of the results of Table 1 reveals that the formation of TAT/CGC^+ base triplets is always more favorable than the formation of TAT/TAT stacks, even for the experiments at pH 7. As the enthalpic contributions of each base triplet stack are similar, the additional stability of TAT/CGC^+ triplets arises from a less unfavorable entropic contribution. This entropic contribution may be the result of several favorable and unfavorable processes. For instance, the lower uptake of sodium ions upon formation of these triplets and the smaller extent of duplex optimization of GC base pairs relative to AT base pairs contribute with favorable entropy, while the protonation of the stem cytosines contributes with unfavorable entropy.

Table 4. Thermodynamic Profiles for the Formation of Base Triplet Stacks

stack	$\Delta G°$ (kcal/mol)	ΔH (kcal/mol)	$T\Delta S$ (kcal/mol)
TAT/TAT	2.1 ± 0.5	24.4 ± 4.9	22.3 ± 8
TAT/CGC^+	4.5 ± 0.8	23.0 ± 3.2	18.5 ± 5
CGC^+/CGC^+		21.7 ± 11	

Comparison of the thermodynamic profiles of the triplexes in the third set reveals that their enthalpy contributions are similar. This is consistent with the results derived from the first two sets and further indicates that the enthalpy contribution of a CGC^+/CGC^+ is also similar to the contributions of the TAT/TAT and TAT/CGC^+ base triplet stacks. Since, the ΔH is mainly due to the formation of base staking interactions, it reflects the simple addition of the contribution of each base triplet stack. Therefore, subtracting the enthalpy contributions of the TAT/TAT and TAT/CGC^+ stacks from the profiles for the folding of AAGGA and AGGAA yields the enthalpy contribution for the formation of a CGC^+/CGC^+ stack. These values are shown in Table 4 and further indicate that the enthalpic contributions for the formation of the base triplet stacks considered in this study are similar. This suggests that binding of the third strand optimizes the base stacking interactions at the duplex and triplex level. Since all the base triplets of this work are composed of two pyrimidines and one purine, complete optimization of each base triplet stack may be able to yield structures with similar enthalpic contributions. On the other hand, the ΔG and ΔS contributions for the formation of these base triplet stacks cannot be calculated by this simplified

(25) Leitner, D.; Schroder, W.; Weisz, K. *J. Am. Chem. Soc.* **1998**, *120*, 7123−7124.
(26) Asensio, J. L.; Lane, A. N.; Dhesi, J.; Bergqvist, S.; Brown, T. *J. Mol. Biol.* **1998**, *275*, 811−822.
(27) Alessi, K. Doctoral Dissertation, New York University, New York, 1995.

procedure because these parameters include additional contributions, such as nucleation, loop formation, sodium and proton uptake or release, and so forth. These latter contributions may be different for this variety of triplexes.

The formation of the triplexes in the third set is more exothermic at pH 6.2 than at pH 7.0. This suggests that optimum stacking of CGC^+ triplets requires low pH conditions to ensure the protonation of the third strand cytosines. This effect is more pronounced in the triplexes containing consecutive cytosines or cytosines next to the loops. This is consistent with previous reports,[20] showing that the pK_a of a third strand cytosine depends on its exposure to the solvent and on the identity of the neighboring bases. For neighboring cytosines, protonation of the second cytosine is more difficult because the presence of a neighboring positive charge decreases its apparent pK_a. The pK_a of a cytosine residue in a single stranded DNA is ~ 4.6,[28] while the pK_a of a cytosine well stacked into the stem of a triplex is ~ 7.4.[20] Cytosine residues partially exposed to the solvent (as in the case of GAAAG) are expected to exhibit a decreased pK_a compared with those of cytosines well stacked into the helix. Thus, the reduction in the pK_a of the cytosines in AGGAA, AAGGA, and GAAAG is consistent with their larger enthalpy difference between pH 6.2 and 7.0.

Thermodynamic Uptake of Counterions. The folding of the "TAT triplexes" and of the control duplexes takes up counterions. This uptake reflects the higher charge density of folded structures compared to that of random coils. As expected, the molecules with more phosphates exhibit a higher uptake of counterions, that is, triplexes versus duplexes. The uptake of counterions decreases at low pH. This effect probably reflects the protonation of their cytosine loops. At low pH, the loops may be protonated and the overall molecule needs to reduce the overall uptake of sodium ions than at pH 7. The "CGC^+ triplexes" release counterions when they form at pH 7 and yielded a small uptake of counterions when folded at pH 5.2. This effect can be explained by the presence of positively charged cytosines, which exclude sodium from the stem of these molecules. The exclusion of sodium is only observed at high pH because these triplexes melt in two sequential transitions at high pH and sodium concentrations, while they melt in monophasic transitions at low pH. Therefore, the release of sodium ions observed at high pH corresponds to the triplex to duplex transition, while the uptake of sodium ions observed at lower pH refers to the coupled triplex to random coil transition. The triplexes containing two consecutive CGC^+ triplets show a smaller uptake of counterions at pH 5.2. This probably reflects the stronger sodium exclusion due to the presence of two consecutive positive charges. The release of counterions upon binding the third strand of the "CGC triplexes" might suggest that these cytosines are protonated only upon docking the third strand onto a duplex, indicating that the changes in the apparent pK_a of these cytosines occur as a result of triplex formation.

Thermodynamic Release of Protons. The "TAT triplexes" and control duplexes take up small amounts of protons upon formation. This uptake probably reflects the protonation of the cytosine loops. Since the loops are not involved in base pairing, protonation of the cytosine loops stabilizes the repulsion between the negatively charged phosphates of the loops, yielding a net

Scheme 3. Proposed Model for the Unfolding of Triplexes Containing CGC^+ Triplets

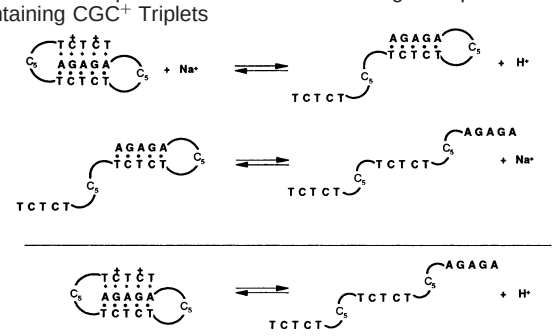

stabilization of the whole molecule. This is consistent with the smaller proton uptake of the duplexes, which contain only one loop. The protonation of the cytosine loops is also consistent with the decrease in sodium uptake observed at low pH; that is, this protonation decreases the overall negative charge density through effective local screening, resulting in the lower uptake of counterions. Furthermore, in the pH range used in our experiments (7.2−5.2), one might expect 0.25−20% of the loop cytosines to be protonated. This will indicate that the triplexes, which contain 10 loop cytosines, may uptake 0.025 to 2 protons or an average of 1 proton for this pH range, in excellent agreement with our experimental results.

At low sodium concentrations, AG5, GAAAG, and AG7 uptake protons in amounts that are consistent with the number of cytosines in their stems. However, at high sodium concentrations, there is a large excess of proton uptake. This excess may be explained by an opposing effect of sodium ions and protons. The presence of sodium destabilizes the triplexes, while the presence of protons stabilizes these molecules. Therefore, as the concentration of sodium increases, more protons are needed to push the equilibrium toward the favorable formation of a triplex. At the molecular level, this can be interpreted as a decrease in pK_a because of the presence of sodium ions around the positively charged cytosines. Because of this pK_a decrease, protonation of the third strand cytosines is induced at a lower pH. At this lower pH, the fraction of cytosine loops that are protonated increases, resulting in a higher uptake of protons. The model shown in Scheme 3 may be adequate to explain the overall folding of the "CGC^+ triplexes". According to this model, the triplex to duplex transition is accompanied by an uptake of sodium, while the duplex to random coil transition is accompanied by a release of sodium ions. When the transitions are coupled (as it occurs at low pHs or low sodium concentrations), these transitions are nearly independent of sodium concentration, as the uptake and release of each half reaction cancel each other. In this model, sodium not only stabilizes the duplex but also destabilizes the triplex. Thus, at high sodium concentrations and pH (the most unfavorable conditions for triplex formation and the most favorable conditions for duplex formation), the overall unfolding reaction starts to separate into two transitions. The relative amounts of proton and sodium ions in the coupled transition depend on their relative amounts in each half reaction. The triplexes with five triplets result in coupled transitions that are independent of sodium concentration, while the larger AG7 triplex takes up some counterions upon formation. This indicates that the higher charge density of the larger duplex part of this triplex is not overridden by the

(28) Zimmer, C.; Luck, G.; Venner, H.; Fric, J. *Biopolymers* **1968**, *6*, 563−574.

exclusion of sodium due to its protonated cytosines. This is consistent with the decrease in charge density of hairpin duplexes due to end effects, which is more pronounced for shorter hairpins.[29,30]

Intramolecular Triplexes and Their Monophasic Transitions. The "TAT/TAT triplexes" always melt in monophasic transitions, as the conditions that stabilize the duplex also stabilize the triplex. The coupled melting of intramolecular triplexes contrasts with the biphasic melting of bimolecular and trimolecular triplexes. This may be a consequence of the lower entropy cost of their overall formation. The favorable entropy change upon the unfolding of the third strand is not large enough to compensate the unfavorable enthalpy of removing the third strand. Our observation that the decoupling of the transitions of AG7 is easier than the decoupling of the transitions of AG5 (data not shown) is consistent with the larger entropy change accompanying the removal of the larger third strand of AG7. The presence of monophasic transitions does not necessarily imply that the Hoogsteen strand is bound more tightly to the purine strand than the Watson−Crick strand. It should rather be interpreted as a $\Delta H-\Delta S$ compensation: the stacking interactions of the overall system are only released when the ΔS of unfolding can pay the price imposed by the large enthalpic penalty of breaking these interactions.

Conclusion

We used a combination of spectroscopic and calorimetric techniques to determine complete thermodynamic profiles accompanying the folding of intramolecular triplexes with different length, strand composition, and sequence. The results show that, under appropriate solution conditions, these triplexes fold in monophasic transitions, driven by a large and favorable enthalpic contribution. The enthalpic contribution is similar for all the base triplet stacks of this investigation and may reflect the binding of the third strand as well as the optimization of duplex stacking interactions. The formation of isometric base triplet stacks with similar enthalpic contributions may have some biological significance because it may facilitate the formation of H-DNA with different sequences. Circular dichroism spectroscopy shows that all triplexes form right-handed "B"-like helices. Melting experiments under a variety of solution conditions show that sodium ions stabilize the "TAT triplexes" but destabilize the "CGC^+ triplexes". In addition, acidic pH stabilizes the "CGC^+ triplexes" by allowing the protonation of the third strand cytosines. The folding of the "CGC^+ triplexes" is consistent with a model in which the triplex to duplex transition is accompanied by an uptake of sodium, while the duplex to random coil transition is accompanied by a release of sodium ions. Therefore, the coupled transitions of these triplexes are nearly independent of sodium concentration but depend on the experimental pH. This may be biologically significant because it provides a way of bypassing the destabilizing effects of physiological salt concentrations to allow specific regions of genomic DNA to fold into "H-DNA" structures. The results also suggest that the monophasic melting of intramolecular triplexes may reflect the lower entropy cost of their overall formation, which cannot override their large and favorable folding enthalpy.

The overall results help to choose adequate solution conditions for the study of intramolecular triplexes containing different ratios of CGC^+ and TAT triplets. The relative stability of these triplexes will depend on their relative amounts of CGC^+ triplets. Our results suggest that, although the stability of these triplets may be greatly reduced under physiological conditions (pH 7.4, [NaCl] $\approx$ 150 mM), they may still form with considerably high stability. Moreover, the results show that it is possible to choose appropriate solution conditions for the monophasic or biphasic melting of intramolecular triplexes. This may be useful to separate the effect of specific factors over the triplex→duplex and duplex→random coil transitions. For example, a drug that stabilizes the monophasic triplex→random coil transition could be further analyzed for its specificity toward the triplex or duplex state by using conditions appropriate for biphasic melting. Moreover, our results are likely to aid in the design of third strands that could effectively target genes involved in human diseases, thereby increasing the feasibility of using the antigene strategy for therapeutic purposes. For example, our results may help in the selection of the sequence, within the gene of interest, which is more likely to form a stable triplex, given the environmental conditions of the cell nucleus.

Acknowledgment. This work was supported by Grant GM42223 (L.A.M.) from the National Institutes of Health and a Blanche Widaman Fellowship (A.M.S.) from UNMC. The editorial assistance of Professor Vinod Labhasetwar is greatly appreciated.

JA026952H

(29) Record, M. T., Jr.; Lohman, T. M. *Biopolymers* **1978**, *17*, 159−166.
(30) Olmsted, M. C.; Anderson, C. F.; Record, M. T., Jr. *Biopolymers* **1991**, *31*, 1593−1604.